Feedback in Low-Luminosity Active Galactic Nuclei

Alberto Rodríguez-Ardila (IAC/Spain; LNA/Brazil); Almudena Prieto (IAC/Spain); Daniel May Nicolazzi (IAG/USP)
Juán Antonio Ontiveros (IAC/Spain); Ximena Mazzalay (MPE/Germany

Abstract

Jet-driven outflows are now recognized as an important ingredient in the active galactic nuclei (AGN) feedback scenario. The effects of such mechanism in low-luminosity radio-quiet AGN (LLAGN, $L_{Bol}/L_{Edd} < 10^{-3}$) is not yet clear. Here, we present challenging results of the feedback mechanisms in two LLAGN by means of SINFONI/VLT spectroscopy. The exquisite angular resolution of tens of parsec/spaxel allows us to unveil at unprecedented detail the extension and morphology of the high-ionization gas mapped through the [Si VI] 19641 Å line. The high-ionization gas (HIG) displays an intricate and complex morphology, following the radio jet and extending to distances of up to 170 pc from the AGN. We measured outflow mass rates of several $M_\odot$ yr^{-1}, similar to those found in powerful radio-galaxies. Our results highlight the importance of the mechanical feedback in LLAGN with low-power radio-jets and shows that its effects to the ISM cannot be underestimated.

NGC 1386

Spatial distribution and morphology of the high-ionization gas

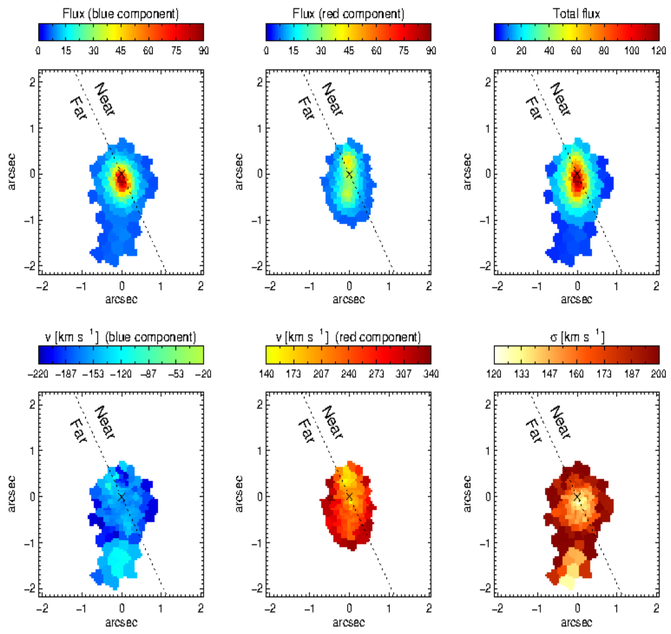

Figure 1. Integrated emission line flux distribution (in units of 10^{-17} erg cm^{-2} s^{-1}) for [SiVI] 19641 Å. The top left and central panels are for the blue and red components of the line, respectively. The right panel is the total flux. The lower panels show the velocity distribution of the blue and red components (left and central panels, respectively), and the velocity dispersion of the line profile (right panel).

Kinematics of the ionized and molecular gas

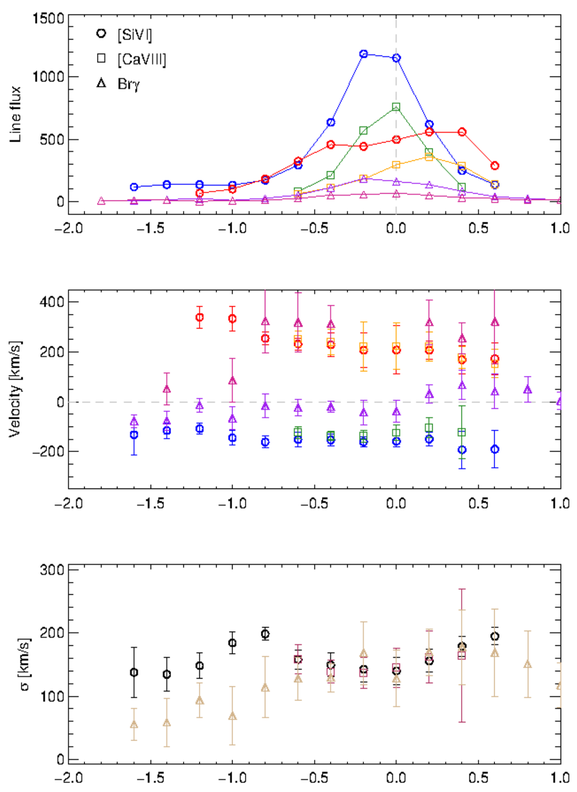

Figure 2. Flux distribution (top, units of 10^{-17} erg cm^{-2} s^{-1}), peak velocity (middle) and velocity dispersion (bottom panel) for [Si VI] (circles), [CaVIII] (squares) and Brγ (triangles) measured in regions of 0.2" × 0.2" along the N–S direction. Negative/positive radii correspond to distances S–N from the nucleus. For lines with splitted components, the results for the blue and red peaks at the corresponding positions are shown.

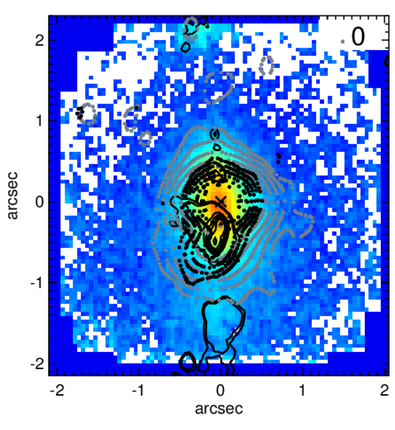

Figure 3. Radio contours (gray and black dotted lines) overplotted to the SINFONI/VLT [SiVI] image. [OIII] HST / WFPC2 contours are represented by the full black line.

ESO 428-G14

Spatial distribution and morphology of the high-ionization gas

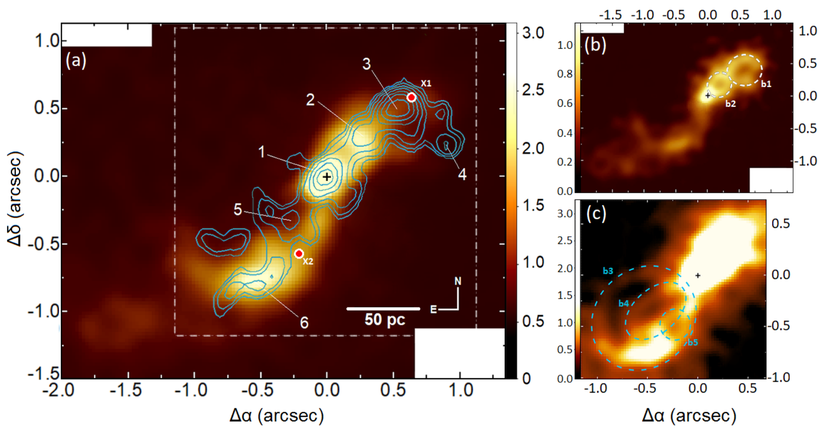

Figure 4. (a): mosaic of two sets of data cubes (DS1) for the [SiVI] emission (total flux of 58±3 x 10^{-15} erg s^{-1} cm^{-2}) overlaid with the VLA 2 cm radio emission (blue contours); the dashed square denotes the VLA FoV and the red dots x1 and x2 are extended Chandra X-ray peaks. (b) Image of Brγ λ21661 Å emission (total flux of 24±1 x 10^{-15} erg s^{-1} cm^{-2}); the dashed ellipses highlight the "helix" in two substructures, b1 and b2. (c): The [Si VI] line from all the combined data cubes (DS2), with smaller FoV and higher S/N. The enhanced contrast shows the faintest structures b3, b4 and b5. The cross marks the AGN position.The flux bar is in units of 10^{-19} erg s^{-1} cm^{-2} $Å^{-1}$.

Kinematics of the ionized gas

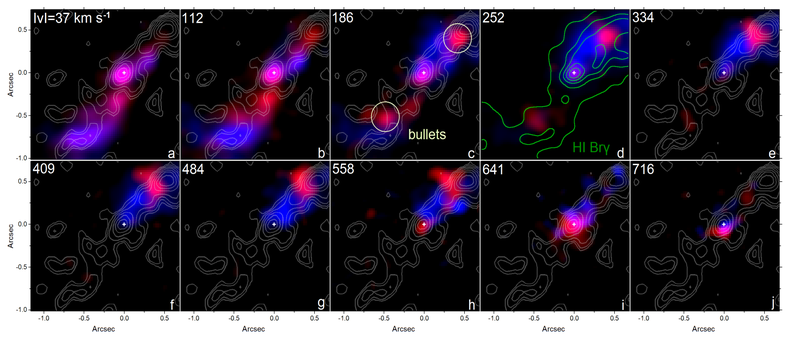

Figure 5. BRV maps (blueshifted and redshifted velocity maps) for the [SiVI] λ19641 Å emission line. The velocity ranges from |v| ≤700 km s^{-1}, with steps of ~75 km s^{-1}. The corresponding absolute velocity of each map is shown at the top. The white and green contours denote the radio and the Brγ emission, respectively. The cross marks the AGN centre.

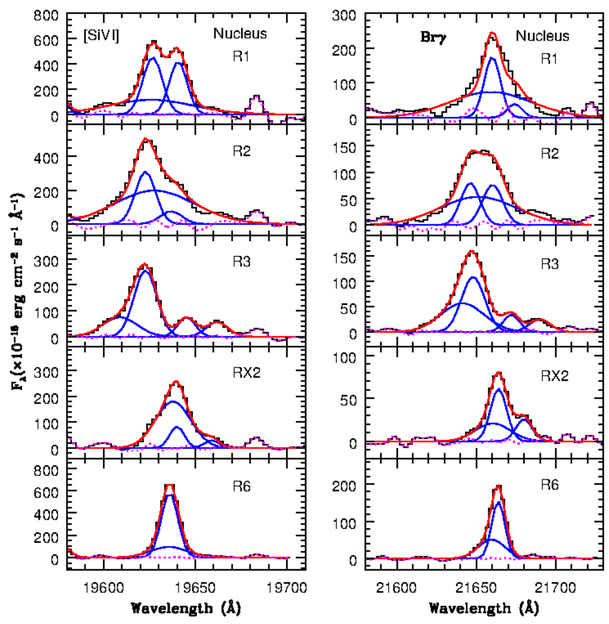

Figure 6. Deblending of the [SiVI] and Brγ lines observed at the nucleus, Region 2 (35 pc NW), region 3 (70 pc NW), region X2 (60 pc SE) and region 6 (85 pc SE). In all cases, the spectra were extracted using an aperture of 0.4" x 0.4" in size. The black histogram is the observed spectrum, the blue lines mark the individual Gaussian components, the red line is the total fit and the dotted magenta line is the residual after subtracting the total fit. The presence of a conspicuous broad component with FWHM > 200 km s^{-1} at all positions evidences a shock component exciting the gas.

Photoionization model results

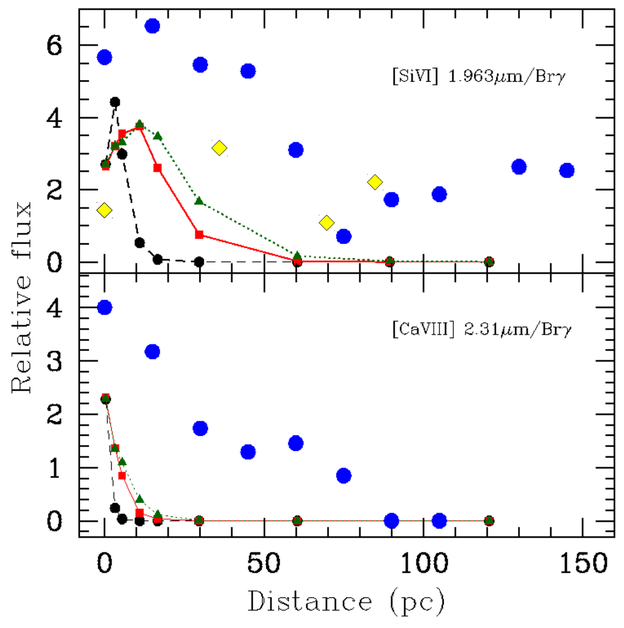

Figure 7. Predicted emission line ratios [SiVI]/Bry (upper panel) and [CaVIII]/Bry (bottom panel) for clouds of density n_e=500 (triangles), n_e=10^3 (squares) and n_e=10^4 cm^{-3} (circles) located at different distances from the centre. Blue points are observations for NGC1386 and yellow diamonds data for ESO428. The ionizing continuum is similar to that of Mathews & Ferland (1987). The intrinsic luminosity above the Lyman limit was set to 2.9 x 10^{42} erg s^{-1} (Fernandez-Ontiveros et al. 2012). Solar abundances from Grevesse et al. (2010) were employed. We measured gas densities > 10^3 cm^{-3} using the Ar^{+3} 4740/4771 Å.

Energetics of the outflowing gas

We use the velocity and the resolved morphology of the outflowing coronal gas associated to the broad components detected in [SiVI] (Figs. 5 & 6) in ESO428 to derive the mass outflow rate, $\dot{M}_{out}$ and the mechanical power injected in the ISM, $\dot{E}_{kin}$ by means of:

$$\dot{M}_{out} = \frac{4}{3}\pi m_p\, n_e\, l\, w\, f\, v_{out}; \quad \dot{E}_{kin} = \frac{1}{2}\dot{M}_{out}(v_{out}^2 + \sigma^2)$$

m_p is the proton mass, n_e is the electronic density, set to 4.2 × 10^3 cm^{-3}; l and w are the length and width radius of each blob, respectively. The filling factor, f , was set to 0.1; v_{out} is the velocity of the peak position of the line relative to the systemic velocity and σ is the gas velocity dispersion. Results obtained are in Table 1.

Table 1. Outflow mass and kinetic power found in ESO428-G14.

Region	l & w (pc)	v_{out} (km s^{-1})	σ (km s^{-1})	n_e (cm^{-3})	$\dot{M}^1_{out}$	$\dot{E}^2_{kin}$
b1	21;15	250	150	4200	3.4	9.2
b2	19;14	200	164	4200	2.3	10.9
b3	50:34	100	150	4200	7.5	7.7
b4	35;19	100	150	4200	2.9	1.5

[1] In units of $M_\odot$ yr^{-1}; [2]Units of $\times 10^{40}$ erg s^{-1}

For NGC 1386, we measured an outflow mass of 5.5 $M_\odot$ yr^{-1}. LLAGNs are fully capable of producing energetic outflows that may significantly impact the ISM in the inner hundreds of parsecs of the central engine!!!

CONCLUSIONS

We show the relevance of the kinetic channel as a major way of releasing nuclear energy to the ISM of LLAGN, up to several percent of the bolometric luminosity, even when driven by radiatively poor radio jets. NGC 1386 and ESO 428-G14 are showcases of this scenario. The derived mass outflow rate, of up to 8 $M_\odot$ yr^{-1} , is similar to that found in powerful radio-loud AGN. Since the energy dumped into the ISM is traced via the high-ionized gas, and given the scales probed (few tens of parsec from the AGN), the reported mass outflow is possibly close to the total amount that is being ejected.